An Ab Initio Study of Lithium Diffusion in Titanium Disulfide Nanotubes

Kevin Tibbetts,* Caetano R. Miranda, Ying S. Meng, and Gerbrand Ceder

Department of Materials Science and Engineering, Massachusetts Institute of Technology, 77 Massachusetts Avenue, Cambridge, Massachusetts 02139

Received June 7, 2007. Revised Manuscript Received August 9, 2007

Using density functional theory (DFT), we have investigated the mobility and insertion potential of Li on single-walled TiS_2 nanotubes as a function of radius. To explore large radii, the nanotube surface is modeled as a curved surface. For small tubes, for which DFT calculations are practical on the complete tube, we find that strain energies, voltages, and activation barriers calculated with the curved surface method are nearly the same as those calculated with a full nanotube. Our results show that, for the range of nanotube radii that are seen experimentally (approximately 50−250 Å), Li diffusion on the nanotube surface is very fast and similar to diffusion on a flat surface. In general, the activation barrier for Li diffusion is 200 meV smaller on the surface than in the bulk, which could result in an improved mobility of Li by a factor of 3000 at room temperature. The effect of tube radius on the Li insertion voltage and migration energy can be explained by the electrostatic repulsion between Li and Ti and by the relaxation of the S atoms.

1. Introduction

Since the discovery of carbon nanotubes in 1991 by Iijima,[1] nanotubes of various other chemistries have been synthesized.[2−13] Inorganic oxide or dichalcogenide nanotubes and nanowires have been widely investigated.[2−10] Chalcogenides of early transition metals often have bulk structures that consist of transition-metal layers sandwiched between layers of anions, such as O, S, or Se,[14] and this structural element is usually preserved in the nanotube, making them structurally somewhat more complex than carbon nanotubes. TiO_2 nanotubes have been used as hydrogen sensors,[15] as electron collectors in dye-sensitized solar cells,[16] and have even displayed photoluminescence properties.[17] WS_2 and MoS_2 nanotubes have been proven as effective solid lubricants.[18] WS_2 nanotubes also display shock wave resistance[19] and have been used as tips in scanning probe microscopy.[20] Superconductivity has been observed in $NbSe_2$ nanotubes.[21]

In this paper, we focus on the potential of inorganic nanotubes as energy storage materials.[22−30] Chen et al.[24] were able to electrochemically charge and discharge open-ended MoS_2 nanotubes with an outside diameter of 50 nm with up to 0.97 wt % hydrogen. Remskar et al.[25] found that bundles of $MoS_{2-x}I_y$ ($x \approx 0$, $y \approx 1/3$) nanotubes of subnanometer diameter could reversibly intercalate Li up to the composition $LiMoS_{2-x}I_y$.[26] H absorption up to 2.5 wt % has been reported for open-ended TiS_2 nanotubes with outer diameter of 30 nm and inner diameter of 10 nm.[27] The same investigators reported chemical intercalation of Li in TiS_2 nanotubes up to the composition $LiTiS_2$.[28] This Li insertion was achieved

* Corresponding author. E-mail: gceder@mit.edu.

(1) Iijima, S. *Nature* **1991**, *354*, 56.
(2) Tenne, R.; Margulis, M.; Genut, M.; Hodes, G. *Nature* **1992**, *360*, 444.
(3) Margulis, L.; Salitra, G.; Tenne, R.; Tallanker, M. *Nature* **1993**, *365*, 113.
(4) Hoyer, P. *Langmuir* **1996**, *12*, 1411.
(5) Kasuga, T.; Hiramatsu, M.; Hoson, A.; Sekino, T.; Niihara, K. *Langmuir* **1998**, *14*, 3160.
(6) Rao, C.; Nath, M. *Dalton Trans.* **2003**, 1.
(7) Tenne, R. *Chem. Eur. J.* **2002**, *8*, 5297.
(8) Remskar, M. *Adv. Mater.* **2004**, *16*, 1497.
(9) Armstrong, R.; Armstrong, G.; Canales, J.; Garcia, R.; Bruce, P. *Adv. Mater.* **2005**, *17*, 862.
(10) Wang, W.; Varghese, O.; Paulose, M.; Grimes, C. *J. Mater. Res.* **2004**, *19*, 417.
(11) Li, N.; Li, X.; Yin, X.; Wang, W.; Qiu, S. *Solid State Commun.* **2004**, *132*, 841.
(12) Tourillon, G.; Pontonnier, L.; Levy, J.; Langlais, V. *Electrochem. Solid State Lett.* **2000**, *3*, 20.
(13) Liu, X.; Zeng, J.; Zhang, S.; Zheng, R.; Liu, X.; Qian, Y. *Chem. Phys. Lett.* **2003**, *374*, 348.
(14) Delmas, C. *Mater. Sci. Eng.* **1989**, *B3*, 97.
(15) Mor, G.; Carvalho, M.; Varghese, O.; Pishko, M.; Grimes, C. *J. Mater. Res.* **2004**, *19*, 628.
(16) Adachi, M.; Marata, Y.; Okada, I.; Yoshikawa, S. *J. Electrochem. Soc.* **2003**, *150*, G488.
(17) Lei, Y.; Zhang, L.; Meng, G.; Li, G.; Zhang, X.; Liang, C.; Chen, W.; Wang, S. *App. Phys. Lett.* **2001**, *78*, 1125.
(18) Rapoport, L.; Fleischer, N.; Tenne, R. *J. Mater. Chem.* **2005**, *15*, 1782.
(19) Rochschild, A.; Cohen, S.; Tenne, R. *App. Phys. Lett.* **1999**, *75*, 4025.
(20) Zhu, Y.; Sekine, T.; Brigatti, K.; Firth, S.; Tenne, R.; Rosentsveig, R.; Kroto, H.; Walton, D. *J. Am. Chem. Soc.* **2003**, *125*, 1329.
(21) Nath, N.; Kar, S.; Raychaudhuri, A.; Rao, C. *Chem. Phys. Lett.* **2003**, *368*, 690.
(22) Arico, A.; Bruce, P.; Scrosati, B.; Tarascon, J.; Schalkwijk, W. *Nat. Mater.* **2005**, *4*, 366.
(23) Cheng, F.; Chen, J. *J. Mater. Res.* **2006**, *21*, 2744.
(24) Chen, J.; Kuriyama, N.; Yuan, H.; Takeshita, H.; Sakai, T. *J. Am. Chem. Soc.* **2001**, *123*, 11813.
(25) Remskar, M.; Mrzel, A.; Skraba, Z.; Jesih, A.; Ceh, M.; Demsar, J.; Stadelmann, P.; Levy, F.; Mihailovic, D. *Science* **2001**, *292*, 479.
(26) Dominko, R.; Arcon, D.; Mrzel, A.; Zorko, A.; Cevc, P.; Venturini, P.; Gabersek, M.; Ramskar, M.; Mihailovic, D. *Adv. Mater.* **2002**, *14*, 1531.
(27) Chen, J.; Li, S.; Tao, Z.; Shen, Y.; Cui, C. *J. Am. Chem. Soc.* **2003**, *125*, 5284.
(28) Chen, J.; Tao, Z.; Li, S. *Agnew Chem. Int. Ed.* **2003**, *42*, 2147.
(29) Tao, Z.; Xu, L.; Gou, X.; Chen, J.; Yuan, H. *Chem. Commun.* **2004**, *18*, 2080.
(30) Jiao, L.; Yuan, H.; Wang, Y.; Cao, J.; Wang, Y. *Electrochem. Commun.* **2005**, *7*, 431.

10.1021/cm0715242 CCC: $37.00
Published on Web 10/03/2007

with chemical intercalation, so no voltage profile is available to compare to the work in this paper. Chen et al. also successfully used TiS_2 nanotubes as the cathode material in rechargeable Mg ion batteries. Mg was intercalated into the nanotubes up to the composition $Mg_{0.49}TiS_2$.[29] Electrochemical Mg insertion was also demonstrated for $VO_{2.32}$ nanotubes with an inner diameter of 15−40 nm and an outer diameter of 60−100 nm.[30]

While the base structure for carbon nanotubes consists of a single graphene sheet rolled to form a tube, inorganic nanotubes are more complicated due to the basic anion−cation−anion triple layer as a structural unit. Considerably more strain is required to roll a triple layer, without shear between the layers, than that required to roll a single layer, making very small inorganic nanotubes unlikely to form. As a result, the nanotube diameters observed for inorganic nanotubes are larger than for carbon nanotubes.[31,32] These structural factors require that models for realistic inorganic nanotubes have several hundreds or even thousands of atoms, far too large for typical ab initio calculations. To reduce the computational burden, we evaluate and use a curved surface technique in this paper. While ab initio studies on carbon nanotubes[33−39] are prevalent, computational studies on inorganic nanotubes are less common.[40−45] Several computational studies have been performed using the density functional tight binding method (DFTB), allowing calculations on larger nanotubes, but with less accuracy than DFT.

In this paper, we examine TiS_2 nanotubes as it is a reasonably well-studied system experimentally. We investigate the electrochemical potential at which Li inserts and its activation barrier for motion as a function of tube radius. The low density of their open structure makes nanotubes not particularly good candidates as electrode materials in rechargeable Li batteries, since energy per unit volume is a crucial performance benchmark for cathode and anode materials. However, this same open structure is likely to allow for fast diffusion of Li. If Li diffusion in nanotubes is considerably faster than that of current electrode materials, then these nanotubes could be used as an additive to other electrode materials to improve Li mobility. Fast Li mobility is crucial when designing a Li battery for high-power applications, such as hybrid electric vehicles, power tools, and emergency power supplies.

There has been some computational research on TiS_2 nanotubes[40−42] using DFTB. Bulk TiS_2 is a semimetal that is stable in the 1T structure type. Ivanovskaya and Seifert[40] determined that the 1T structure type is also the stable form for nanotubes and showed that single-walled TiS_2 nanotubes of any chirality are semiconductors with a band gap that decreases with decreasing radius. Ivanovskaya et al. later reported a more detailed band structure for TiS_2 nanotubes[41] to show that the metal−semiconductor transition in TiS_2 occurs at approximately 10 layers.

Little is known about how the properties of inorganic nanotubes change with the radius of the nanotube. Computational methods could be useful in obtaining this knowledge, but this is difficult with standard methods due to the size of the unit cell. To overcome this difficulty, we model the nanotube surface with a curved surface. By explicit comparison between results on a small tube and a curved surface, we find that local properties of the surface, such as Li hopping, are similar to those of nanotubes. By using the curved surface approach, we can study nanotubes of any radius of curvature and thus investigate nanotubes of the size that are produced experimentally.

Our calculations show that for radii above a critical radius, approximately 50 Å for TiS_2 nanotubes, most kinetic and thermodynamic properties of single-walled nanotubes are similar to those for a single TiS_2 triple-layer sheet.

2. Computational Details

2.1. Methodology. Calculations were carried out using density functional theory (DFT) as implemented in the Vienna Ab initio Simulation Package (VASP).[46] We have used the generalized gradient approximation (GGA) of Perdew−Burke−Ernzerhof (PBE) to treat the exchange and correlation interaction. Projector-augmented-wave (PAW) potentials were used[47,48] with valence states $3d_34s_1$ for Ti, $3s_22p_4$ for S, and $1s_12s_12p_1$ for Li.

Structural parameters for a TiS_2 sheet, consisting of a sulfur−titanium−sulfur triple layer, were determined using a three atom unit cell with a 15 Å vacuum layer. Atomic positions as well as unit cell shape and volume for this structure were relaxed using a $15 \times 15 \times 4$ Monkhorst−Pack *k*-point mesh until the forces on all atoms were less than 0.03 eV/Å. Constant curvature was applied to the relaxed TiS_2 sheet to create curved surfaces like those shown in Figure 1.

Any periodicity along the length of the nanotube (or the curved surface) can be used in our calculations. For voltage and strain calculations, the minimal cell containing one Ti in the direction of the nanotube axis (∼3.45 Å) was used. A cell twice as long was used for activation barrier calculations. For a radius of 9.5 Å, these unit cells contained 36 and 72 atoms, respectively. For all other radii, the unit cells contained 60 and 120 atoms. When relaxing the curved surfaces, the unit cell shape and volume were kept fixed and only the atomic positions of the S atoms were allowed to change. Inspection of the forces on the Ti atoms and tests where Ti atoms were allowed to relax showed that freezing the Ti atoms did not have a significant effect on the results. Calculations were converged until all forces were less than 0.03 eV/Å with a Monkhorst−Pack *k*-grid of $1 \times 1 \times 6$.

(31) Rao, C. N. R.; Satishkumar, B. C.; Govindaraj, A.; Nath, M. *Chem. Phys. Chem.* **2001**, *2*, 78.
(32) Rao, C. N. R.; Govindaraj, A. *Nanotubes and Nanowires*; Royal Society of Chemistry: London, UK 2005.
(33) Srivastava, D.; Menion, M.; Cho, K. *Comput. Sci. Eng.* **2001**, *3*, 42.
(34) Meunier, V.; Kephart, J.; Roland, C.; Bernholc, J. *Phys. Rev. Lett.* **2002**, *88*, 075506.
(35) Lee, Y.; Nardelli, M.; Marzari, N. *Phys. Rev. Lett.* **2005**, *95*, 076804.
(36) Mori, H.; Ogata, S.; Li, J.; Akita, S.; Nakayama, Y. *Phys. Rev. B* **2006**, *74*, 165418.
(37) Dubay, O.; Kresse, G. *Phys. Rev. B* **2003**, *67*, 035401.
(38) Cheng, H.; Cooper, A.; Pez, G.; Kostov, M.; Piotrowski, P.; Stuart, S. *J. Phys. Chem. B* **2005**, *109*, 3780.
(39) Liu, Y.; Nishimura, N.; Otani, Y. *Comput. Mater. Sci.* **2005**, *34*, 173.
(40) Ivanovskaya, V. V.; Seifert, G. *Solid State Commun.* **2004**, *130*, 175.
(41) Ivanovskaya, V. V.; Seifert, G.; Ivanovskii, A. *Semiconductors* **2005**, *39*, 1058.
(42) Enyashin, A.; Ivanovskii, A. *Inorg. Mater.* **2005**, *41*, 1118.
(43) Enyashin, A.; Seifert, G. *Phys. Status Solidi* **2005**, *242*, 1361.
(44) Seifert, G.; Terrones, H.; Terrones, M.; Jungnickel, G.; Frauenheim, T. *Phys. Rev. Lett.* **2000**, *85*, 146.
(45) Verstraete, M.; Charlier, J. J. *Phys. Rev. B* **2003**, *68*, 045423.
(46) Perdew, J. P. *Phys. Rev. B* **1996**, *54*, 16533.
(47) Blochl, P. E. *Phys. Rev. B* **1994**, *50*, 17953.
(48) Kresse, G.; Joubert, D. *Phys. Rev. B* **1999**, *59*, 1758.

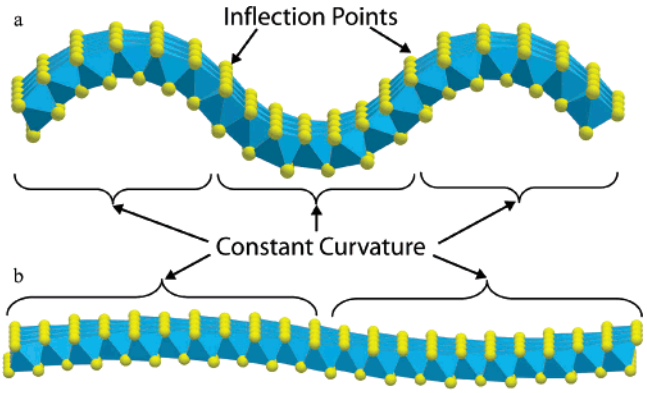

Figure 1. Curved surfaces with radius of curvature of 9.5 Å (a) and 100 Å (b).

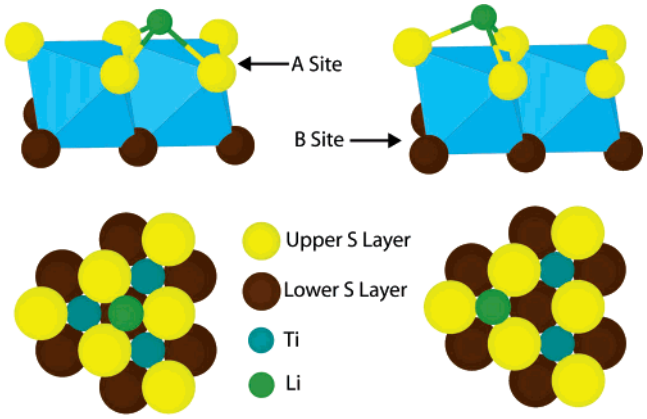

Figure 2. A and B type Li site on the surface of a TiS_2 sheet.

To contrast the activation barrier for Li motion on the curved surface and in the bulk, a bulk activation barrier calculation was performed on a $2 \times 2 \times 2$ supercell, which gives about the same distance between the migrating Li and its image as that on the curved surface. These bulk calculations were converged until all forces were less than 0.03 eV/Å, with a $4 \times 4 \times 4$ Monkhorst–Pack *k*-point mesh.

Activation barriers for Li motion were calculated using the nudged elastic band (NEB) method[49,50] with nine intermediate images. We performed a test using 19 intermediate images, yielding results within 2 meV of the results obtained with nine intermediate images, verifying that nine images is sufficient for these calculations. The NEB is an efficient method to determine the extrema of the energy surface along the minimum energy path between a given initial and final set of positions. Li insertion/absorption voltages were calculated with the procedure described in refs 51 and 52.

2.2. Structure and Lithium Positions. Bulk TiS_2 forms the CdI_2-1T structure, which consists of layers of Ti atoms octahedrally coordinated by S atoms. These triple layers (S–Ti–S) are separated by a van der Waals gap and stacked such that the titanium atoms project on top of each other. Lithiation occurs by insertion of Li into the octahedral sites in the van der Waals gap. The octahedral site is formed by three S atoms from each of the layer above and below the Li atom. There is also a tetrahedral Li site, in which Li is coordinated by three S atoms from one triple layer and one S atom from the other triple layer. Diffusion of Li in bulk Li_xTiS_2 occurs by migration from one octahedral site to another, passing through this tetrahedral site.[53]

Table 1. Li Insertion Voltage and Activation Barrier on a Curved Surface and Full Nanotube with Radius of 9.5 Å

radius, Å	9.4	9.5
sample	curved surface	full nanotube
strain energy, meV/formula unit	145	125
Li voltage outside, V	1.292	1.305
Li voltage inside, V	1.353	1.356
activation barrier for Li diffusion, meV	261	270

The two possible sites for Li on the surface of a TiS_2 sheet or curved surface can be related to the bulk sites they are derived from. In both sites Li is coordinated by three S atoms at a distance of approximately 2.4 Å. In the A site, derived from the bulk tetrahedral site, the Li atom sits above a S atom from the bottom layer of the sheet, at a distance of approximately 3.4 Å from three Ti atoms. In the B site, corresponding to the bulk octahedral site, the LiS_3 tetrahedron shares its sulfur triangle with a Ti–S octahedron and is directly above a Ti atom at a distance of 2.8 Å. Both of these surface sites are shown in Figure 2.

3. Results

To verify whether nanotubes can be approximated by curved surfaces, we compare the calculated strain energy, Li voltage, and Li migration barrier for a true nanotube with a radius of 9.5 Å to the values calculated for a curved surface with the same radius of curvature (Table 1). Strain energy is defined as the energy difference per formula unit between the curved surface (or nanotube) and the sheet. We find that the strain energy of the curved surface is 20 meV (14%) larger than for the nanotube. This is a property we do not expect to be accurately reproduced by the curved surface. Strain energy depends on the complete structure of the tube, while the curved surface approximation is intended to model local nanotube properties.

The Li insertion voltage and activation barrier depend mainly on the local environment of the Li atom and, as a result, are expected to be less affected by the curved surface approximation. For the tube with a 9.5 Å radius, the lithium voltage is 13 mV (1%) higher than for the curved surface. The activation barrier is found to be accurate to within 9 meV (3%). The accuracy of the curved surface approximation should improve for larger radii of curvature, as a larger radius of curvature results in less strain and thus less variation from a sheet. The accuracy of this approximation should also improve with the larger unit cells that were used for all other curved surface calculations, as a larger unit cell for the curved surface is affected less by the inflection points where the curvature inverts.

We also compared the electronic properties of the curved surface with those of the full nanotube. The electron localization function (ELF) is a measure of the electron localization based on the density of electrons of the same spin.[54–56] The ELFs for the nanotube and the curved surface

(49) Mills, G.; Jonsson, H.; Schenter, G. *Surf. Sci.* **1995**, *324*, 305.
(50) Jonsson, H.; Mills, G.; Jacobsen, K. *Classical and Quantum Dynamics in Condensed Phase Simulations*; World Scientific Publishing Co.: Hackensack, NJ, 1998.
(51) Aydinol, M.; Kohan, A.; Ceder, G. *J. Power Sources* **1997**, *68*, 664.
(52) Zhou, F.; Coccocioni, M.; Morgan, D.; Marianetti, C.; Ceder, G. *Phys. Rev. B* **2004**, *70*, 235121.
(53) Mendizabal, F.; Contreras, R.; Aizman, A. *J. Phys. Condens. Matter* **1997**, *9*, 3011.
(54) Becke, A. D.; Edgecombe, K. E. *J. Chem. Phys.* **1990**, *92*, 5397.
(55) Silvi, B.; Savin, A. *Nature (London)* **1994**, *371*, 683.
(56) Savin, A.; Nesper, R.; Wengert, S.; Fässler, T. F. *Angew. Chem., Int. Ed. Engl.* **1997**, *36*, 1808.

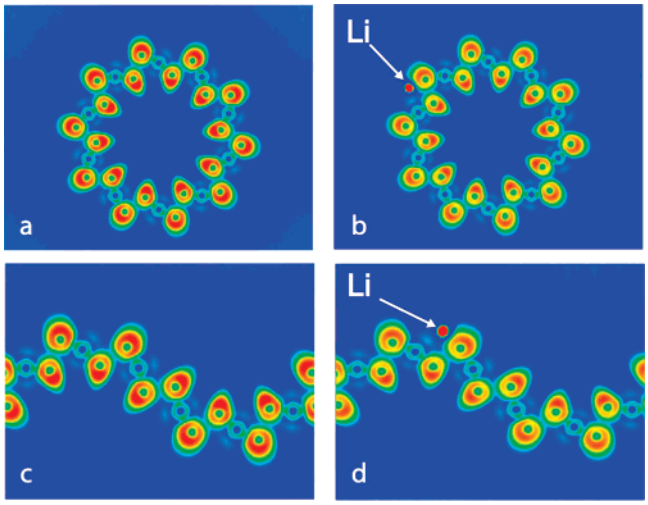

Figure 3. Electron localization function for a full nanotube without Li (a) and with Li (b) and for a curved surface without Li (c) and with Li (d).

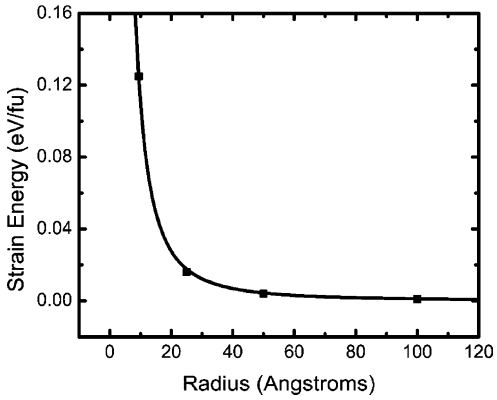

Figure 4. Calculated (points) strain energy of a TiS_2 curved surface as a function of radius. The solid line is the function A/r^2, where $A = 11$ eV Å^2 per formula unit.

with and without Li are shown in Figure 3. These images show that, in the vicinity of the Li atom, the ELF for the curved surface is similar to that for a full nanotube. In addition, inside the nanotube, the ELF is elliptical, in contrast with the outside electronic environment, where the ELF functions are spherical around the S atoms. The curvature method is able to reproduce the inner and outer ELF characteristics of the full nanotube, lending further support for the approximation of a nanotube by a curved surface.

The calculated strain energy versus radius is shown in Figure 4 for TiS_2 curved surfaces. This data can be fitted with the form A/r^2, expected for elastic strain energy. Above a radius of 50 Å, the strain energy is very small, less than 1 meV per formula unit.

We also compared the Li insertion voltage in the A and B sites (data not shown). For most curved surfaces, the A site is more stable than the B site. For the flat sheet and surfaces with large radius of curvature, the difference is small, ~40 mV. For Li on the inside of the curved surface there is a transition at small radii where the B site becomes more stable. Figure 5 shows that the Li insertion voltage both inside and outside of the nanotube decreases as the radius decreases. The horizontal line displays the voltage for a sheet, 1.525 V. For most radii the voltage is slightly lower on the inside of the tube compared to the outside, though the opposite is true at the smallest radii.

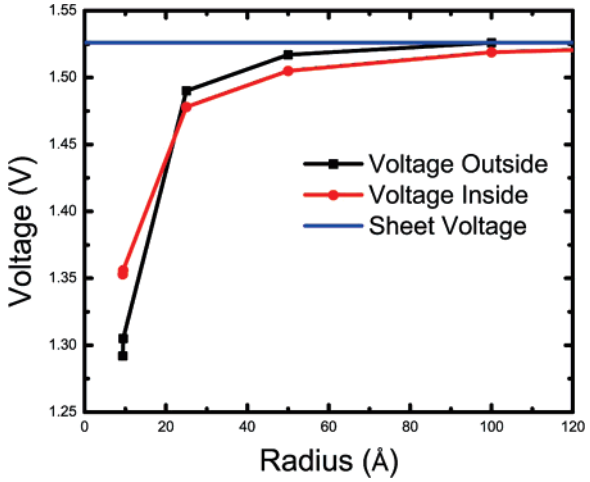

Figure 5. Li voltage as a function of radius for Li inserted in the A site both inside and outside of the curved surface. The horizontal line is the voltage for a TiS_2 sheet with no curvature.

Voltage calculations are performed by comparing the energy of $TiS_2 + xLi$ to the energy of Li_xTiS_2. As the Li composition, x, increases, the nearest Li−Li distance decreases. The stronger Li−Li interaction results in a voltage that decreases with increasing composition. The voltages shown in Figure 5 are for a single Li in our supercells. Due to the shape of the supercell, this results in a short Li−Li distance (3.5 Å) in the direction of the nanotube axis but large Li−Li distance in the other direction. Typically one would expect a more homogeneous distribution of Li−Li distances to minimize the electrostatic repulsion between them.[57,58] As a result, our cell shape may give a lower voltage then what would be observed from a homogeneous cell with the same Li concentration. By comparing the voltage for TiS_2 sheets with various homogeneous Li distributions to those with a short Li−Li distance, we determined that the voltage calculated using our supercells probably more reflects a nanotube with ~25% Li concentration. At a similar Li concentration in the bulk ($Li_{0.25}TiS_2$), the calculated voltage is approximately 2.2 V. The experimentally measured open circuit voltage for $Li_{0.25}TiS_2$ is approximately 2.4 V.[59] Calculations on a flat sheet showed an average voltage of 0.9 V for the reaction

$$Li + TiS_2 \rightarrow LiTiS_2$$

compared to an average voltage of 1.9 V for the same reaction in the bulk material.

Using the NEB method,[49,50] we find that the path by which Li migrates between two A sites passes through a B site (shown in Figure 6). This is opposite to bulk Li_xTiS_2, where Li diffuses through a tetrahedral (A) site when migrating between two octahedral (B) sites (Figure 7).

The maximum energy along the Li^+ migration path (the activation barrier) was calculated for various radii of the tube and is shown in Figure 8a,b. The energy along the Li migration path in bulk TiS_2 or on the outside of large

(57) Ceder, G.; Van der Ven, A. *Electrochim. Acta* **1999**, *45*, 131.
(58) Arroyo y de Dompablo, M. E.; Van der Ven, A.; Ceder, G. *Phys. Rev. B* **2002**, *66*, 064112.
(59) Whittingham, M. S. *Science* **1976**, *192*, 1126.

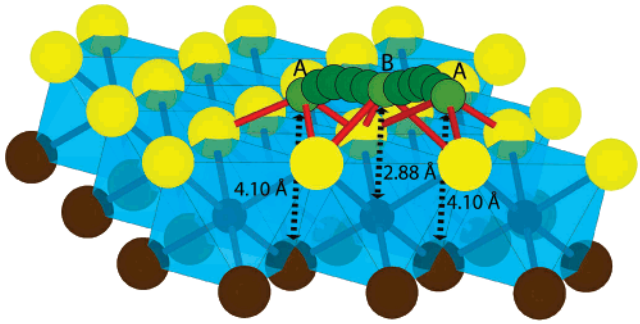

Figure 6. The Li diffusion path between two A sites on the surface of a TiS_2 sheet goes through a B site.

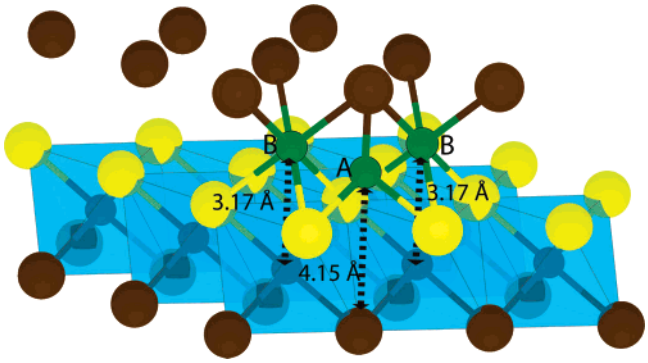

Figure 7. The Li diffusion path in TiS_2 bulk between two 6-fold coordinated B sites goes through a 4-fold coordinated A site.

nanotubes is shown in Figure 8a. The barrier on the sheet is approximately 180 meV, which is 200 meV lower than that in the bulk. The barriers on curved surfaces are notably higher than those on a sheet. While for a radius of curvature of 100 Å the barrier is only slightly larger than that for a sheet, on a tube with a radius of 25 Å the activation barrier increases to 220 meV. The difference of 200 meV between the activation barrier in the bulk and on the 100 Å nanotube will have a large effect on Li transport, since the diffusion coefficient in general varies exponentially with the activation barrier through an Arrhenius-like formula:

$$D \propto e^{(E_A/kT)}$$

At room temperature a difference of 200 meV would result in a change in Li mobility by a factor of 3000. The energy along the diffusion path for the smallest nanotubes (Figure 8b) is considerably different for the path inside and outside of the nanotube, especially at the midpoint of the diffusion path. The activation barrier is 270 meV for Li on the outside and 220 meV for Li on the inside of the 9.5 Å tube. In either case, the activation barrier on nanotubes is considerably lower than that in the bulk but larger than that on a sheet with no curvature. There is little difference between the activation barrier on the curved surface and on a real 9.5 Å radius nanotube.

4. Discussion

We find that the strain energy of a tube can be well represented by A/r^2, the expected form for the elastic bending of a continuum sheet. For tubes with radius greater than 50 Å, the strain energy is small and less than 1 meV/formula unit. Our values for the strain energy are somewhat lower

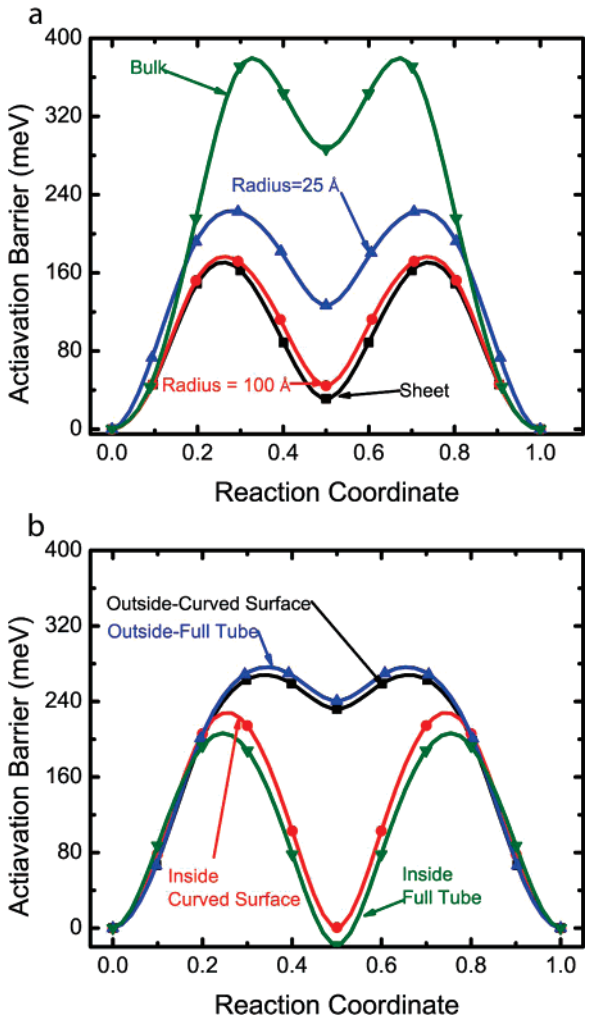

Figure 8. (a) Energy along the Li migration path in bulk TiS_2 and on the outside of surfaces with large radius of curvature. (b) Same as part a but inside and outside of a full nanotube with a radius of 9.5 Å and a curved surface with a radius of 9.4 Å. For the curved surfaces and nanotube, reaction coordinates 0 and 1 correspond to site A, and reaction coordinate 0.5 to site B. For the bulk, this assignment is inverted.

than those obtained in previous DFTB studies.[40,41] This is true for the curved surfaces and full nanotubes and is likely due to a more complete relaxation obtained with DFT than what is achieved by DFTB, rather than a problem with the curved surface method.

We find that the Li insertion voltage for nanotubes is smaller than that for a flat sheet, which in turn is considerably below the voltage for bulk Li insertion. The variation of the Li voltage with the radius of the tube can be understood by considering the electrostatic interaction between Li^+ and the other ions. Figure 9 shows the Li position on the surface of a TiS_2 sheet, on the outside of a curved surface, and on the inside of a curved surface. As the radius of curvature decreases, the triangle of S atoms that defines the Li site on the outside of the curved surface expands. As a result, the Li atom must move closer to the curved surface to maintain the optimal distance from the S atoms (Figure 9b). This moves the Li atom closer to the Ti layer, increasing the electrostatic repulsion between the positively charged Li and Ti ions. The balance between the S−Li interaction and the Ti−Li interaction determines the optimum position of the Li. The increased electrostatic interaction with the Ti atom

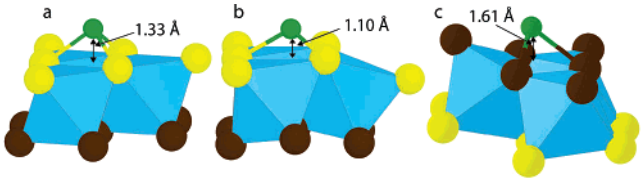

Figure 9. Li environment on the surface of a TiS_2 sheet (a) and outside (b) and inside (c) a curved surface with a radius of 9.4 Å. The distance between the Li atom and the plane of S atoms is shown for each case. Light (yellow online) circles represent S atoms on the outside of the tube. Dark (black online) circles are S on the inside.

results in an increased site energy for Li and thus a reduction in voltage.

This is not the case when Li is on the inside of the curved surface. The triangle of S atoms compresses, causing the Li atom to move away from the surface (Figure 9c). As a result, the lithiation voltage on the inside for the smallest tubes is higher than on the outside. For radii larger than about 25 Å, the main cause for the decrease in Li voltage at the inside position is the inability of the S atoms to relax when the Li atom is inserted. The S atoms are compressed on the inside of the surface and as a result are more constrained than on the flat sheet or outside the curved surface. We tested this hypothesis by calculating Li insertion voltages while S atoms were kept fixed to the positions they have in an unlithiated tube. Under this constraint, the calculated Li voltage of 1.4 V at the inside position of a 25 Å curved surface is the same as on the flat sheet.

The contribution of Li−Ti electrostatics and sulfur relaxation can also be used to explain the increasing activation barrier with decreasing radius. The increase of the barrier due to electrostatic repulsion is apparent in the shape of the energy profile along the migration path in Figure 8a,b. The largest energy difference between the path on the outside of a curved surface and the one on the flat sheet occurs at the B site, which is the midway point of the hop (reaction coordinate ≈ 0.5 in Figure 8a). At this position, the Li−Ti distance is smallest as the Li atom is directly above the Ti atom. This is confirmed by the data in Figure 10, which shows the distance between the migrating Li atom and the nearest Ti atom. When Li is *outside* the nanotube, this minimal Li−Ti distance decreases with decreasing radii, thereby increasing the energy for Li at this position. While the maximum energy along the migration path does not occur at the B site, we believe that the increase in B site energy lifts up the energy surface and is the major factor in controlling the activation barrier.

Activation barrier calculations were performed using a cell twice as long as the cell used for voltage calculations, representing a dilute Li concentration of approximately 5%. It is well-known that the Li voltage will decrease with increasing concentration, but the effect of concentration on the activation barrier for Li diffusion is not as clear. This depends on the energy of the system with Li in the activated state relative to the energy with Li in the stable site. We have shown in this paper that for TiS_2 the electrostatic interaction between Li and Ti are crucial in determining the activation barrier for Li diffusion. As the Li concentration is increased, the valence on the Ti atoms is reduced. This will reduce the strength of the Li−Ti interaction, which is most influential when Li is in the activated state, possibly resulting in a lower activation barrier.

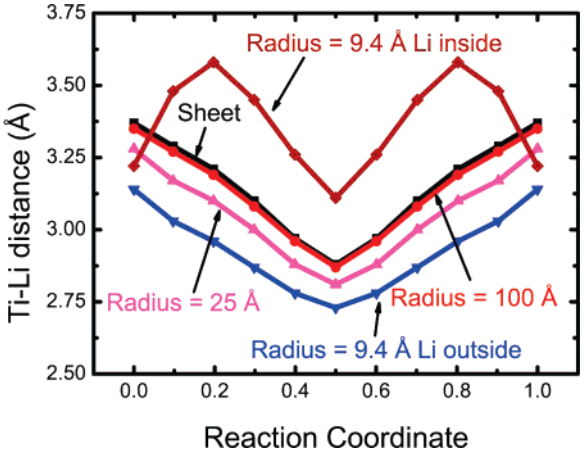

Figure 10. Smallest Ti−Li distance along the Li migration path on nanotubes with various radii of curvature.

Calculations discussed in this paper were performed on nanotubes and curved surfaces with armchair chirality. Nanotubes with other chiralities will have Li sites and diffusion paths slightly different than those discussed in this paper. Essentially the orientation of bonds relative to the nanotube axis will be different. This will likely result in small quantitative differences, but qualitatively the results should be the same.

While the results presented in this paper are for TiS_2 nanotubes in the 1T structure type, it may be possible to draw some more general conclusions about the lithiation voltage and Li mobility on nanotubes of other chemistries. It is the *strain* in the inside and outside surface that indirectly seems to control the change in lithiation voltage from the flat sheet. Tensile strain increases the effective anion−anion distance on the surface, drawing the Li atom closer in. Whether this has a strong effect on the potential depends on the nature and distance to the other cations. For a Li insertion site with a Ti^{4+} cation directly below (the B site in our structure) the effect of curvature is the most pronounced. For structure types where the preferred Li site is not in close proximity to other cations, the effect of curvature on the lithiation energy may be significantly less. Overall, curvature effects on the voltage are small above a radius of 25−50 Å and can be well approximated by the lithiation voltage of the flat sheet, which should facilitate future investigations of inorganic nanomaterials for battery applications. Most inorganic tubes have radii well above 25 Å, making this finding particularly relevant.

Our results confirm the speculation that nanotubes may function as fast diffusion paths for ions such as Li. Even though the activation barrier increases with decreasing radius it remains well below the value in bulk, even for the smallest tubes we tested. The voltage on the nanotube must match the voltage of the primary electrode material in order for the Li sites on the nanotube to be active during Li diffusion. Thus, TiS_2 nanotubes would only improve Li diffusion of electrode materials with a maximum operating voltage near ~1.5 V.

While computational resources limit this study to single-walled nanotubes, experimental nanotubes are likely to be

multiwalled. The lithiation voltage and migration on the outside or inside of multiwalled tubes will likely behave as shown here for single walled tubes, as long as their surfaces are similar. Li diffusion on the surface of a nanotube is dominated by the curvature-induced stress in the surface below a critical radius, but it is similar to Li diffusion on the surface of a flat sheet above this radius. It is unlikely that thick, multiwalled tubes can consist of concentric layers of connected TiS_2 sheets that one would obtain by bending a thick sheet without bond breaking. When the tube wall becomes too thick, it is likely that layers will slip or contain dislocations to relieve the strain. Such strain relief will significantly reduce the effects of curvature on the Li reaction energy and activation barrier. The critical thickness at which dislocation generation becomes favorable in epitaxial layers has been derived for planar systems[60] and for spherical nanoparticles,[61] but to our knowledge, no such study has been undertaken for nanotubes or nanowires.

In multiwalled tubes, Li can also diffuse in layers below the surface. For epitaxially connected layers (e.g., derived from bending a slab without bond breaking), one would expect the activation energy for Li migration to be close to the bulk value, as the coordination and environments are similar. In this case, the B site would be the stable site and diffusion would be from a B site to an A site to another B site. Relaxation of the activated state in the subsurface layers may slightly reduce its energy from the bulk value. In other related materials such small relaxation effects have been shown to be important.[62] Lithiation of multiwalled tubes is likely to occur by direct insertion of Li in the ends of open-ended tubes or migration along the surface, where the activation barrier is likely to be significantly lower than inside the tube, followed by hops into the tube through defects. As the sites inside the tube will have higher potential, they will fill before the surface sites are full, leaving the surface free for fast Li ion transport. This combination of low-voltage, high-mobility surface sites with higher voltage internal sites seems to be the ideal combination to make a high rate electrode material.

5. Conclusions

In summary, we find that Li diffusion on a flat surface of TiS_2 is considerably faster than in the bulk. Curved surfaces maintain this mobility advantage and are similar to a flat sheet in their thermodynamic and kinetic properties until the radius of curvature approaches 25−50 Å, at which point the activation barrier starts to increase with decreasing radius. But even for the smallest tubes, the Li migration barrier is well below the value in the bulk. Li reacts with TiS_2 tubes in the voltage range 1.3−1.5 V, which is considerably below the bulk TiS_2 voltage of 2.2 V, making single-walled TiS_2 nanotubes uninteresting for cathode applications. However, it is possible that oxide tubes or sulfide tubes with later transition metals have a higher voltage, making them a better match for common cathode materials. As the voltage inside multiwalled tubes is likely to approach that of the bulk, they may be better suited as electrode materials.

The variation of Li voltage and migration barrier can be well-rationalized by considering the electrostatic repulsion with the Ti cations and the strain on the S atoms that form the outside and inside surface. When Li is on the outside of the tube, the tensile strain in the outer sulfur layer pulls the Li closer to the Ti in the center of the tube, thereby decreasing the voltage. On the inside of the tube, it is the compressive strain in the S layer preventing their relaxation that increases the voltage with decreasing radius. Except for the smallest tubes, the Li voltage is higher on the outside of the tube than on the inside, though the difference is small and less than the magnitude of the Li−Li interactions that control the variation of voltage with Li composition. Hence, it is likely that at the limit of lithiation both the inside and outside of a tube will be partially occupied.

The activation barrier for Li migration is similarly controlled by electrostatics. The closer Li approaches Ti cations along the migration path, the higher the activation barrier.

Our results indicating very high mobility for Li across the surface of TiS_2 nanotubes are likely to hold for other nanotube chemistries and support the exciting prospect of these materials as additives for high-rate Li battery electrodes.

Acknowledgment. This work was supported by the MRSEC Program of the National Science Foundation under Grant No. DMR 02-13282, by the Assistant Secretary for Energy Efficiency and Renewable Energy, Office of FreedomCAR and Vehicle Technologies of the U.S. Department of Energy under Contract No. DE-AC02-05CH11231, with the Lawrence Berkeley National Laboratory. Additional computer resources were provided by the National Partnership for Advanced Computing Infrastructure (NPACI) at the San Diego Supercomputer Center.

CM0715242

(60) Ariel, N.; Ceder, G.; Sadoway, D. R.; Fitzgerald, E. A. *J. Appl. Phys.* **2005**, *98*, 023516.
(61) Balasubramanian, S.; Ceder, G.; Kolenbrander, K. D. *J. Appl. Phys.* **1996**, *79*, 4132.
(62) Kang, K.; Ceder, G. *Phys. Rev. B* **2006**, *74*, 094105.